Available online at www.sciencedirect.com
ScienceDirect
Journal of Sound and Vibration 301 (2007) 560–575
JOURNAL OF SOUND AND VIBRATION
www.elsevier.com/locate/jsvi

Reconstruction of a distributed force applied on a thin cylindrical shell by an inverse method and spatial filtering

M.C. Djamaa[a,*], N. Ouelaa[a], C. Pezerat[b], J.L. Guyader[b]

[a]*Laboratoire de Mécanique & Structures (LMS), Université du 8 mai 45, BP. 401, 24000 Guelma, Algérie*
[b]*Laboratoire de Vibrations & Acoustique (LVA), INSA de Lyon, Bat. Antoine de Saint-Exupéry, 25 bis, avenue Jean Capelle, 69621 Villeurbanne, Cedex, France*

Received 19 August 2006; received in revised form 12 October 2006; accepted 16 October 2006
Available online 22 December 2006

Abstract

The localization and the magnitude of acting steady-states forces resulting from the dynamic response of a cylindrical shell are investigated. The derivatives present in the equation of motion are expressed in terms of displacements using finite-difference schemes. Displacements of the structure are introduced into the equation of motion in order to calculate the distribution of these forces. Numerical simulations show that when the force distribution is calculated using well-defined displacements, the exact position of the force is easily determined. However, when the displacements are mixed with uncertainties, noise appears and the real force is relatively inaccurate. In order to handle this instability in the inverse problem, a regularization method based on signal processing techniques such as windowing and filtering in the spatial wavenumber domain should be performed. Numerical examples that illustrate the regularization process show that when the local filtering is applied to the force distribution, calculated from noisy data, reasonable results are obtained. Experiments are performed on a cylindrical shell in order to measure its velocities. Unfortunately, using the displacements derived from measured velocities, high sensitivity to the noise in the measurements is observed. Overall, the experimental identification gives also good results when the same technique of filtering is applied to the force distribution.

1. Introduction

In many practical situations, the direct measurements of internal or external sources acting on a vibrating structure are very difficult to perform. However, it is easy to predict the position and magnitude of these sources by using indirect methods that are based on the measured dynamic response of the structure at discrete points. These kinds of problems are very sensitive to noise in the input data and can introduce large deviations from the exact solution of the inverse problem.

The cylindrical shells, as structures used in various engineering applications, are subjected to various excitations. The vibro-acoustic behavior of this kind of structures has been studied by several researchers [1–3]. However, few papers dealt with the inverse problem in the case of shell structures rather than with

*Corresponding author. Tel.: +213 75 54 90 07; fax: +213 37 21 58 50.
E-mail address: mc_djamaa@yahoo.fr (M.C. Djamaa).

0022-460X/$ - see front matter © 2006 Elsevier Ltd. All rights reserved.
doi:10.1016/j.jsv.2006.10.021

plates. Anthony and Willliams [4] used surface pressure and normal velocity for thin shells and plates to determine the structural intensity which allows locating the force position. Zhang and Mann III [5,6] used the FFT to calculate the structural intensity and the force distribution for plates and presented their results before and after windowing and filtering. Nedjade and Singh [7] estimated the structural intensity for plates using Spatial Fourier Transforms and an ideal band-pass filter centered at the structural wavenumber k from spaced dynamic response measurements. De Araújo et al. [8] proposed a remote identification method of impact forces acting on tubes. The problem was then regularized by a signal processing technique which allows the separation of the multiple wave sources. Nakaggiri and Suzuki [9] proposed a finite-elements formulation to identify the nodal forces by introducing the nodal uncertain displacements of a flat plate. Karlsson [10] focused his study on the sensitivity of the inverse process. He proposed a semi-experimental approach to identify unknown harmonic force amplitudes arising from the response at discrete measurement points. Liu et al. [11] preferred the application of Kalman filter with a recursive estimator to determine the input force from the measured systematic responses by an inverse algorithm. Pezerat and Guyader [12–14] developed the RIFF method (in French Résolution Inverse Filtrée et Fenêtrée) to localize the excitation sources acting on beams and plates using a finite-difference method and computed the force distribution from noisy displacement field. To reduce the noise effect, a regularization step based on filtering and windowing of the force distribution was performed. Djamaa et al. [15] proposed an extension of the RIFF method to the cylindrical shells and highlighted the possibility to reconstruct the force distribution from radial exact displacements only at the ring frequency and far above. However, it was shown that at low frequencies, the simplifications are not allowed because the curvature has a significant effect on the shell behavior. Consequently, the axial and tangential deformations must be measured and introduced in the computing process. In order to optimize the acoustic design of vibrating flat plate, Yang and Koopmann [16] calculated the equivalent force from the measurement of radiated sound power.

This paper addresses the effect of the uncertainties on the reconstructed force and introduces numerical simulations at various frequencies to locate the force position over the surface of a cylindrical shell. By using well-defined filter parameters, positive results were obtained after windowing and filtering in the spatial wavenumber of the noisy force distribution. The same approach gives also positive results when using measured velocities of a region of the shell to compute the force distribution.

2. Formulation of the direct problem

The equation of motion of a circular cylindrical shell (Fig. 1), subject to a force applied along the radial direction takes the following form:

$$\frac{Eh}{1-\nu^2}L\begin{Bmatrix} u \\ v \\ w \end{Bmatrix} + \rho\omega^2 h\begin{Bmatrix} u \\ v \\ w \end{Bmatrix} = -\begin{Bmatrix} 0 \\ 0 \\ F_w \end{Bmatrix}. \tag{1}$$

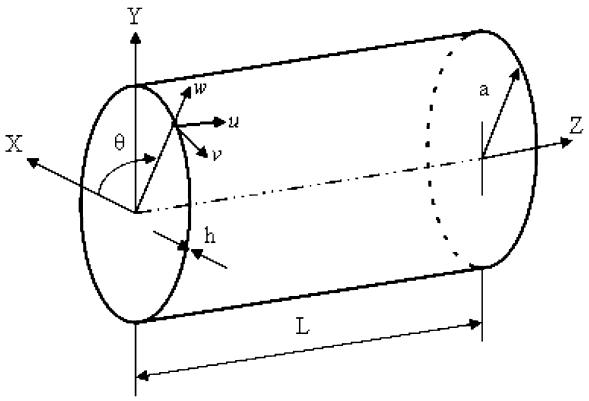

Fig. 1. Geometry of the structure.

Here E is the Young's modulus, h is the thickness, v is the Poisson's ratio, (u, v, w) are the displacements, ρ is the shell density, ω is the angular frequency, F_w is the radial force, a is the shell radius and L is Donnell's operator.

The displacements (u, v, w) are computed by the modal method:

$$u = \sum_{\alpha=0}^{1}\sum_{n=0}^{\infty}\sum_{m=1}^{\infty}\sum_{j=1}^{3} A^a_{nmj} D_{nmj} \sin(n\theta + \alpha\pi/2)\cos(m\pi/L),$$

$$v = \sum_{\alpha=0}^{1}\sum_{n=0}^{\infty}\sum_{m=1}^{\infty}\sum_{j=1}^{3} A^a_{nmj} E_{nmj} \cos(n\theta + \alpha\pi/2)\sin(m\pi/L),$$

$$w = \sum_{\alpha=0}^{1}\sum_{n=0}^{\infty}\sum_{m=1}^{\infty}\sum_{j=1}^{3} A^a_{nmj} \sin(n\theta + \alpha\pi/2)\sin(m\pi/L). \quad (2)$$

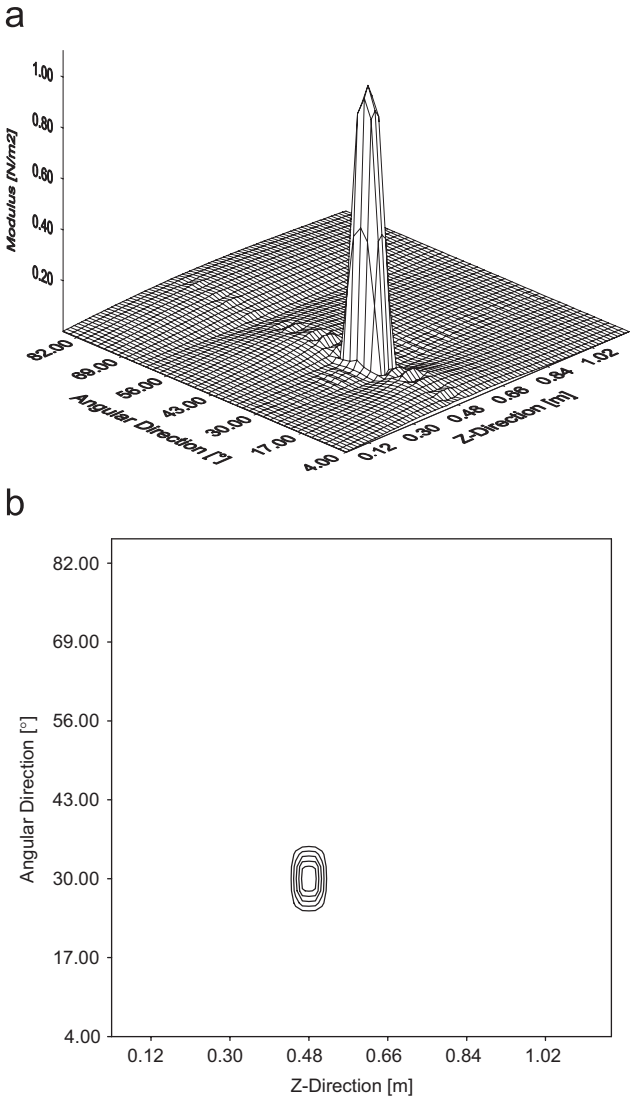

Fig. 2. Force distribution computed from exact displacements at 160 Hz: (a) 3D presentation, (b) map contours.

Here α is an integer, its even values indicate the symmetric modes and the odd values the anti-symmetric modes, n and m are the circumferential and longitudinal mode number, respectively, j is the mode type, D_{nmj} and E_{nmj} are the eigenvector components and A_{nmj} are the modal amplitudes.

3. Calculation of the force distribution

In the absence of the axial and tangential forces, the equation of motion (1) takes the following form:

$$\frac{Eh}{1-\nu^2}\left(-\left(\frac{v}{a}\frac{\partial u}{\partial z}\right)-\left(\frac{1}{a^2}\frac{\partial v}{\partial \theta}\right)-\left(\frac{w}{a^2}\right)+\frac{h^2}{12}\left(\frac{\partial^4 w}{\partial z^4}+\frac{2}{a^2}\frac{\partial^4 w}{\partial z^2\partial\theta^2}+\frac{1}{a^2}\frac{\partial^4 w}{\partial\theta^4}\right)\right)+\rho h\omega^2 w=-F_w. \tag{3}$$

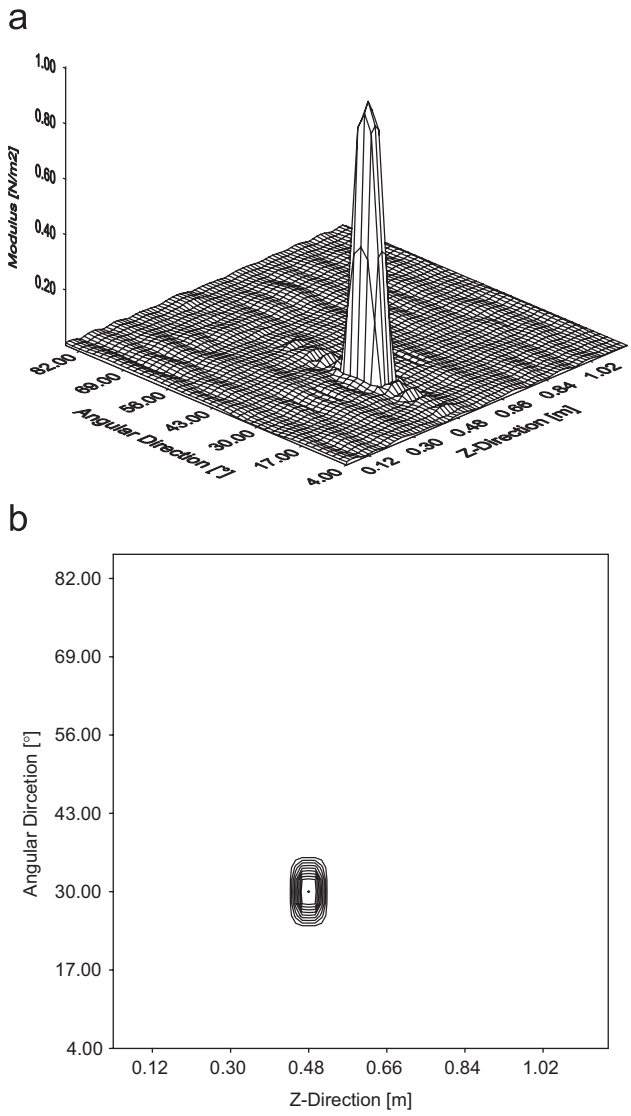

Fig. 3. Force distribution computed from exact displacements at 2128 Hz: (a) 3D presentation, (b) map contours.

The proposed method permits to approximate the fourth-order derivatives in Eq. (3) using finite-difference schemes as follows:

$$\frac{\partial^4 w}{\partial z^4} \Leftrightarrow \delta_{ij}^4(z) = \frac{1}{\Delta_z^4}(w_{i+2,j} - 4w_{i+1,j} + 6w_{i,j} - 4w_{i-1,j} + w_{i-2,j}),$$

$$\frac{\partial^4 w}{\partial \theta^4} \Leftrightarrow \delta_{ij}^4(\theta) = \frac{1}{\Delta_\theta^4}(w_{i,j+2} - 4w_{i,j+1} + 6w_{i,j} - 4w_{i,j-1} + w_{i,j-2}),$$

$$\frac{\partial^4 w}{\partial z^2 \partial \theta^2} \Leftrightarrow \delta_{ij}^4(z,\theta) = \frac{1}{\Delta_z^2}\frac{1}{\Delta_\theta^2}(w_{i+1,j+1} - 2w_{i+1,j} + w_{i+1,j-1} - 2w_{i,j+1} + 4w_{i,j} - 2w_{i,j-1} + w_{i-1,j+1} - 2w_{i-1,j} + w_{i-1,j-1}). \quad (4)$$

The complete inverse resolution takes into account the deformations $\partial u/\partial z$ and $\partial v/\partial \theta$. In our case, they are deduced from the finite-difference schemes as follows:

$$\frac{\partial u}{\partial z} \Leftrightarrow \frac{1}{2\Delta_z}(u_{i+1,j} - u_{i-1,j}) \text{ and } \frac{\partial v}{\partial \theta} \Leftrightarrow \frac{1}{2\Delta_\theta}(v_{i,j+1} - v_{i,j-1}). \quad (5)$$

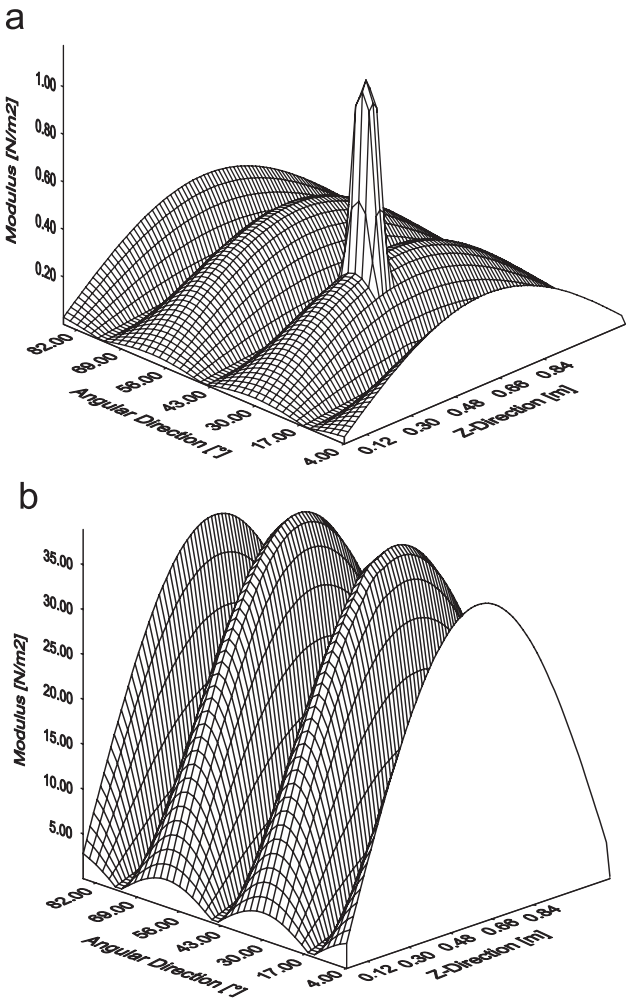

Fig. 4. Force distribution computed from exact displacements at 178.7 Hz (resonance mode): (a) with structural damping of 0.01, (b) with structural damping of 0.0001.

Here Δ_z and Δ_θ denote the distance between two consecutive points in the longitudinal and circumferential directions, respectively.

The deformations $\partial u/\partial z$ and $\partial v/\partial\theta$ must be measured at each point of the structure's surface by strain gauges. These measurements may deem difficult to achieve when the number of points is very high.

By substituting Eqs. (4) and (5) into Eq. (3), the force distribution is computed for each frequency as follows:

$$F_{ij} = \frac{E(1+j\eta)h}{1-\nu^2}\left(\frac{\nu}{2a\Delta_z}(u_{i+1,j}-u_{i-1,j}) + \frac{1}{2a^2\Delta_\theta}(v_{i,j+1}-v_{i,j-1}) + \frac{w_{ij}}{a^2} + \frac{h^2}{12}(\delta^4_{ij}(z)+\frac{2}{a^2}\delta^4_{ij}(z,\theta)+\frac{1}{a^4}\delta^4_{ij}(\theta))\right) - \rho h\omega^2 w_{ij}. \quad (6)$$

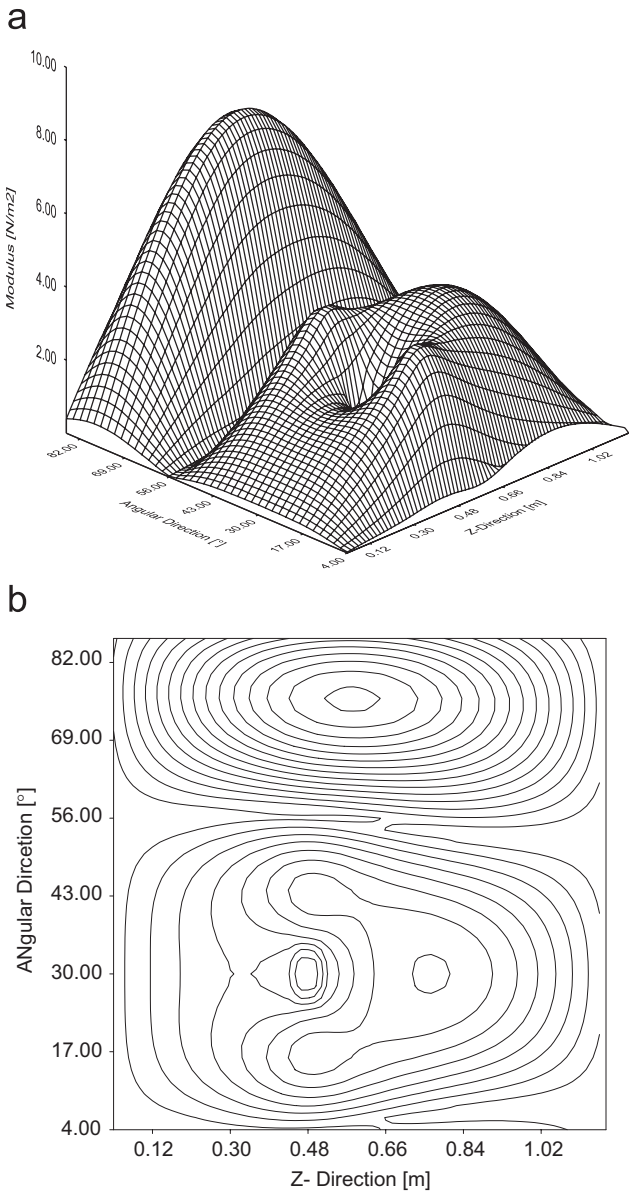

Fig. 5. Force distribution computed from exact radial displacements at 160 Hz: (a) 3D presentation, (b) map contours.

To rebuild the force acting at point (i,j), this technique requires the measurement of radial displacements at 13 points and four translations around the considered point.

4. Numerical results

The numerical simulations were made on a cylindrical shell with dimensional characteristics ($l = 1.2\,\mathrm{m}$, $a = 0.4\,\mathrm{m}$ and $h = 3\,\mathrm{mm}$), Young's modulus $E = 2.068.10^{11}\,\mathrm{N\,m^{-2}}$, density $\rho = 7850\,\mathrm{kg\,m^{-3}}$, Poisson ratio $v = 0.29$ and structural damping $\eta = 1\%$.

The shell is excited by a distributed force of $1\,\mathrm{N\,m^{-2}}$ between 0.45 and 0.51 m along the axial direction and between 26° and 34° along the angular direction. The displacements are computed with the modal method over 81×46 grid points which cover an area of 1.2 m by 90°.

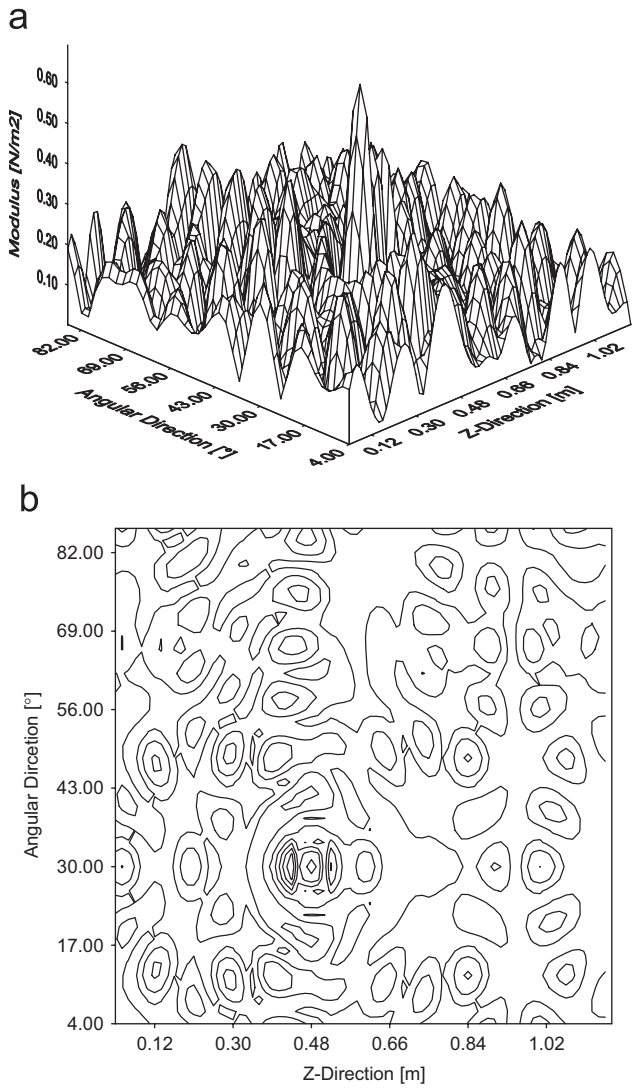

Fig. 6. Force distribution computed from exact radial displacements at 2128 Hz: (a) 3D presentation, (b) map contours.

The ring frequency, as a characteristic of cylindrical shells, is defined by

$$f_a = \omega_a/2\pi = \frac{1}{2\pi}\sqrt{\frac{1}{a}\left(\frac{E}{\rho(1-\nu^2)}\right)}. \tag{7}$$

4.1. Reconstruction of the force from exact displacements

Using a shell that is excited at a frequency of (160 Hz) and a ring frequency of (2128 Hz), the force distribution is calculated using Eq. (6) and the results are presented in Figs. 2 and 3. In both cases, a peak corresponding to the true position of the applied force appears clearly. At the resonance frequency of 178.7 Hz and for the same structural damping (1%), the amplitudes of the displacements become eight times greater than those obtained at 160 Hz but the localization of the force remains always possible (Fig. 4(a)). However, as

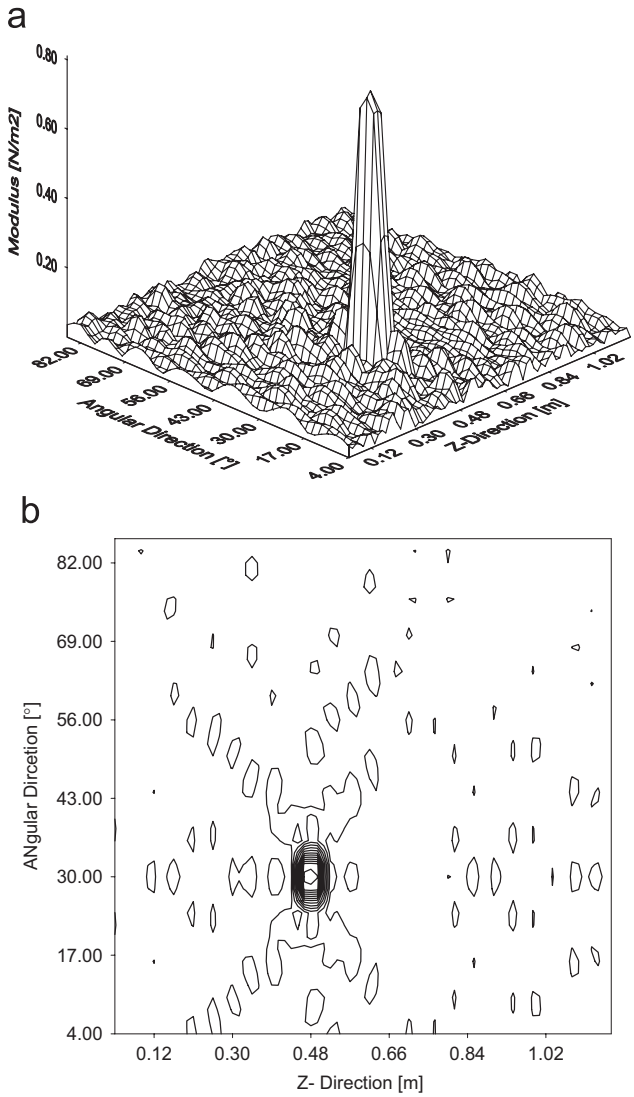

Fig. 7. Force distribution computed from exact radial displacements at 4000 Hz: (a) 3D presentation, (b) map contours.

shown in Fig. 4(b), when the structural damping takes negligible values (0.0001 for example), the amplitudes of displacements on the entire surface of the cylinder becoming several times (6.10^4 times) greater than those away from resonance. For this reason, the true force is lost.

4.2. Force reconstruction from radial exact displacements

As can be seen from Eq. (3), if the deformations are assumed to be very small in comparison with the shell radius, their influence on the reconstructed force can be neglected. This assumption will have a considerable impact if it is to be true at all frequencies since, in this case, the radial displacements can be easily measured by the Scanning Laser Vibrometer. Figs. 5–7 show the force distributions calculated from exact radial displacements at 160, 2128 and 4000 Hz, respectively. It is clear that at frequencies below the ring frequency, the force is completely dominated by a significant distortion. This distortion is due to a very strong coupling between the radial motion and the in-plane one. Consequently, the simplifications made in the shell operator,

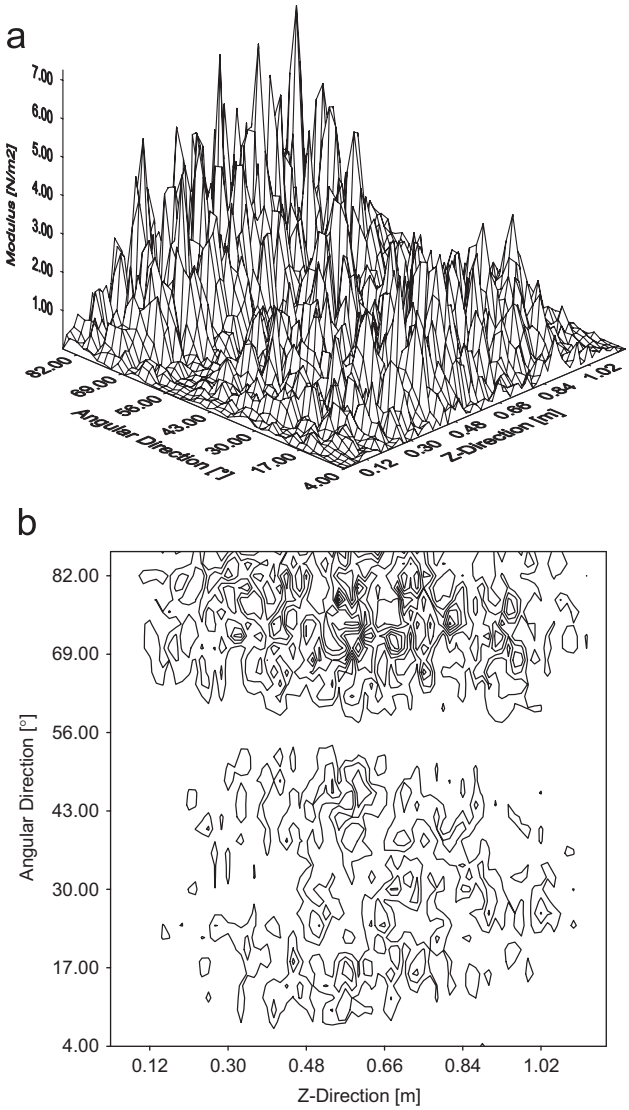

Fig. 8. Force distribution computed from noisy displacements at 160 Hz with 1% of noise in module and phase: (a) 3D presentation, (b) map contours.

are not allowed and the axial and tangential deformations must be measured and introduced in the computing process. However, it is possible to reconstruct the force at the ring frequency and far above since the cylindrical shell will behave as a flat plate as the radius of the curvature is large in comparison to the flexural wavelength.

4.3. Force distribution from noisy displacements

To simulate the displacements with uncertainties (measured data), errors are voluntarily added to the exact displacements. For example, the noisy radial displacement is calculated by the following

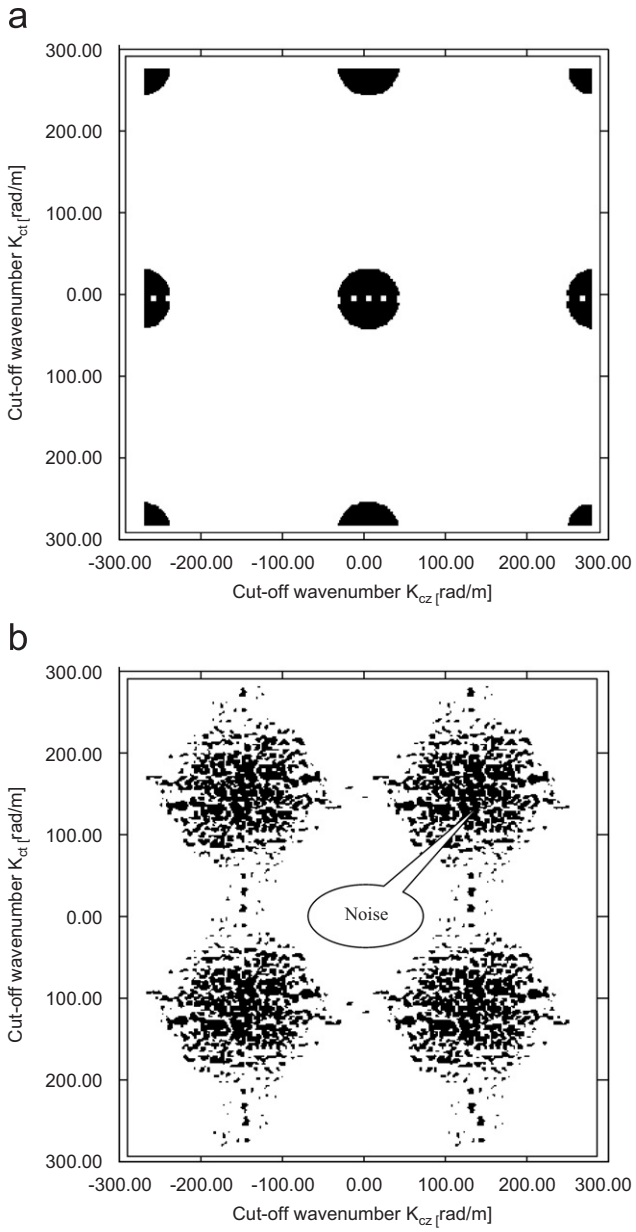

Fig. 9. Map contours of two-dimensional spatial Fourier transforms of the force distribution at 160 Hz: (a) from exact displacements, (b) from noisy displacements.

expression:

$$w^{\text{noisy}} = w^{\text{exact}}(\Delta w + e^{j\Delta\theta}). \tag{8}$$

Here Δw is a Gaussian random real number with (mean = 1 and $\sigma = 1\%$) and $\Delta\theta$ is another Gaussian random real number with (mean = 0 and $\sigma = 1^\circ$).

The noisy force distribution reconstructed at 160 Hz is presented in Fig. 8. We can see that the noise dominates the real force which is amplified by the derivatives of fourth order.

5. Regularization technique

The present section is concerned with the regularization of the inverse problem in order to reduce the effect of uncertainties associated with the input data on the reconstructed force. The proposed approach is similar to the one used in Refs. [5,13] for plates, but extended to cylindrical shells.

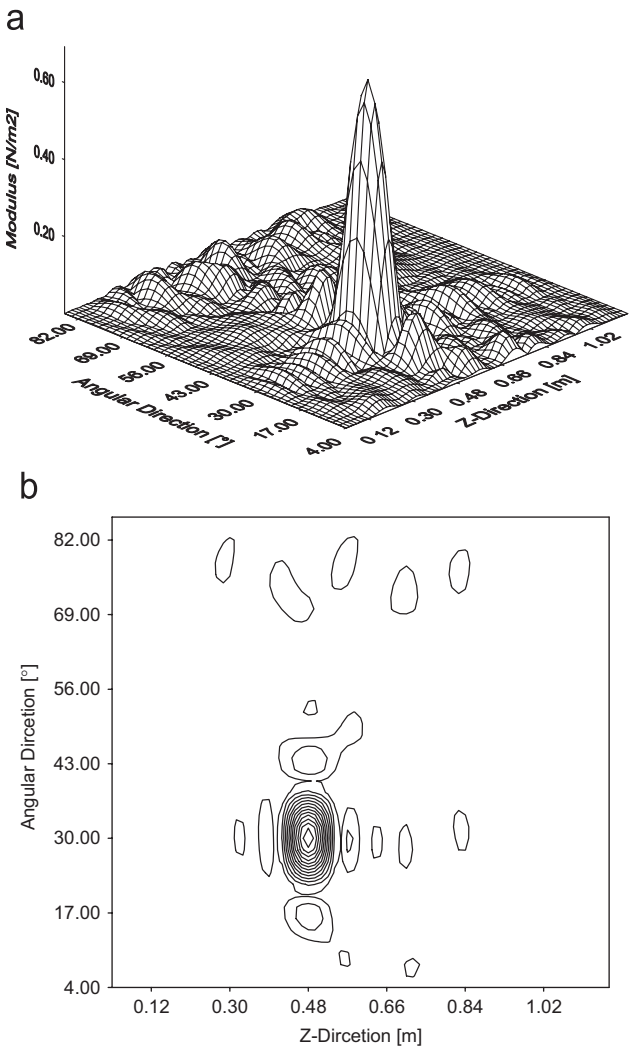

Fig. 10. Force distribution reconstructed after windowing and filtering at 160 Hz, the cut-off wavenumber along both directions is 50 rad m^{-1} and the form factor of the filter is equal to 4: (a) 3D presentation, (b) map contours.

By a simple filtering, residual forces can appear at the structure boundaries following the limitation of the spatial domain. In this case, windowing must be applied before filtering in order to smooth out the effects of these forces. This can be done by multiplying the noisy force distribution by the window function along both directions

$$\overset{\text{windowed}}{F(z,\theta)} = \overset{\text{original}}{F(z,\theta)}\,\psi(z,\theta). \tag{9}$$

The window function is defined along the z-direction for example as:

$$\begin{aligned} &\psi(z) = 0.5(1-\cos(\pi z/\beta)) \quad \text{for} \quad z < \beta, \\ &\psi(z) = 1 \quad \text{for} \quad \beta \leqslant z \leqslant l-\beta, \\ &\psi(z) = 0.5(1-\cos(\pi(z-l+2\beta)/\beta)) \quad \text{for} \quad z > l-\beta. \end{aligned} \tag{10}$$

Several simulations resulted in determining the Hanning half-window (β) making it possible to remove the residual forces at the structure boundaries. Its value is estimated equal to the half cut-off wavelength of the filter ($\lambda_c/2$).

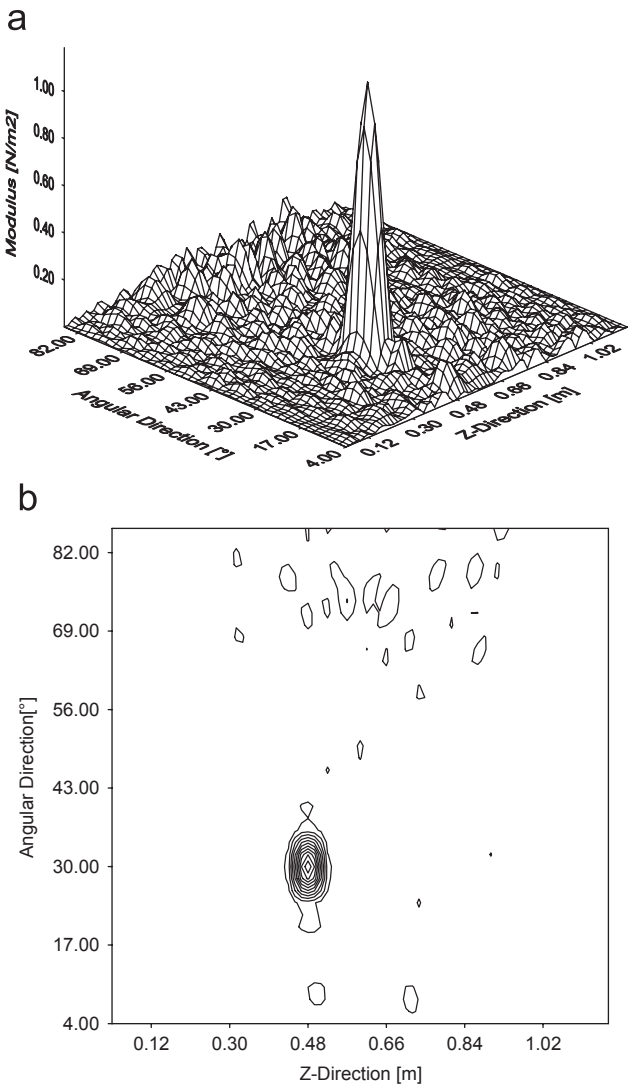

Fig. 11. Force distribution reconstructed after windowing and filtering at 160 Hz, the cut-off wavenumber along both directions is 50 rad m^{-1} and the form factor of the filter is equal to 1: (a) 3D presentation, (b) map contours.

The regularization method is based on the use of an ideal filter to remove aberrant forces in the wavenumber domain. The transfer function of the filter is defined as

$$\begin{aligned} &\hat{h}(k) = 1 \quad \text{for} \quad k \in [-k_c;\, +k_c\,], \\ &\hat{h}(k) = 0 \quad \text{otherwise.} \end{aligned} \tag{11}$$

Here k_c is the cut-off wavenumber ($k_c = 2\pi/\lambda_c$).

The spatial response of the filter along both axial and circumferential directions is defined as the product of two $\sin c$ functions as given below

$$h(z,\theta) = \frac{1}{4\pi^2}\int_{-k_{cz}}^{+k_{cz}}\int_{-k_{c\theta}}^{+k_{z\theta}} \hat{h}(k_z)\hat{h}(k_\theta)\mathrm{e}^{\mathrm{j}k_z z}\mathrm{e}^{\mathrm{j}k_\theta a\theta}\,\mathrm{d}k_z\,\mathrm{d}k_\theta \frac{\sin(k_{cz}z)\sin(k_{c\theta}a\theta)}{\pi^2 z a\theta}. \tag{12}$$

The filtering procedure consists of the discrete convolution product between the windowed force distribution calculated by Eq. (9) and the spatial response of the filter calculated by Eq. (12)

$$F_{ij}^{\text{filtred}} = \Delta_z a \Delta_\theta \sum_{k=0}^{N_z-2}\sum_{l=0}^{N_\theta-2} F_{kl}\, h((i-k)\Delta_z, (j-l)a\Delta_\theta). \tag{13}$$

In this case, the filtered force distribution should be computed with all the components of the noisy force distribution. In order to conserve the local aspect of the finite-difference method, a low-pass filter with finite spatial response defined as a $\sin c$ function limited by a Hanning window is used in both directions. It will have the zero value outside the window ($-\beta$ to β) along the z-direction and It will have the same value outside the window ($-\gamma$ to γ) along the angular direction. The spatial response of the filter has the following expression:

$$h(z,\theta) = \left(1+\cos\left(\frac{k_{cz}z}{2f_z}\right)\right)\left(1+\cos\left(\frac{k_{c\theta}a\theta}{2f_\theta}\right)\right)\frac{\sin(k_{cz}z)\sin(k_{c\theta}a\theta)}{4\pi^2 z a\theta}. \tag{14}$$

Here k_{cz} and $k_{c\theta}$ are the cut-off wavenumber along the axial and circumferential directions, respectively. f_z and f_θ are the "Form Factors of the Filter" along the axial and circumferential directions, respectively.

As shown in Fig. 9(b), the noise appears at high wavenumber domain. The main difficulty lies in choosing the cut-off wavenumber in both directions. An optimum cut-off wavenumber is estimated as the greatest wavenumber for which the overlap between the two-dimensional spatial Fourier transforms (Fig. 9(a) and (b))

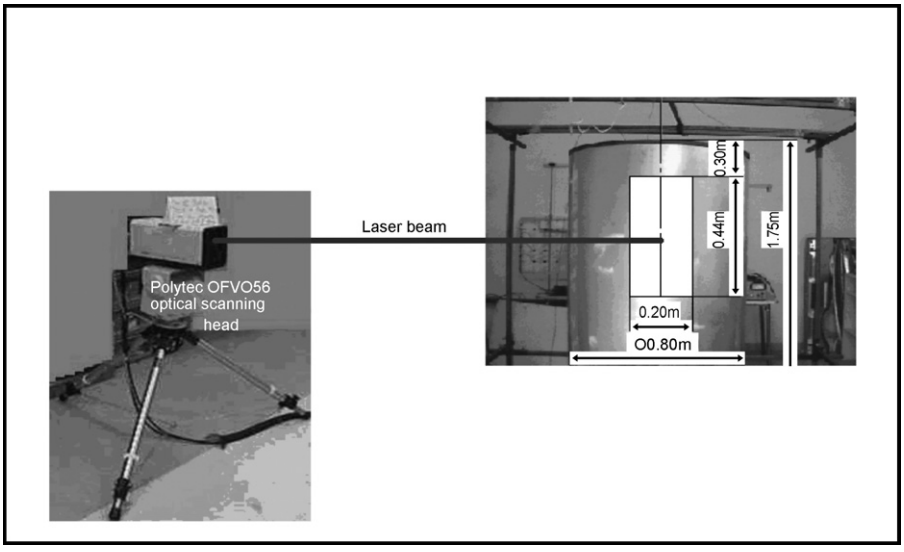

Fig. 12. Experimental setup.

calculated at a specified frequency is obtained. A cut-off wavenumber that is either too small or too big may result in erroneous results.

The ''Form Factor of the Filter'', is defined as the ratio of the half-length of the Hanning window and the cut-off wave length. This parameter is adjusted according to the nature of the force which will be rebuilt. For a large distributed force, the value of this parameter is estimated to be equal to 4 and for a single point force, it is estimated to be equal to 1.

Fig. 10 shows the force distribution after local filtering for ($k_{cz} = k_{c\theta} = 50\,\mathrm{rad\,m^{-1}}$) and ($f_z = f_\theta = 4$). A peak corresponding to the exact location of the force appears and the noise is completely eliminated. Since the distributed force is applied on a limited area, the same result is obtained with ($f_z = f_\theta = 1$) where the reconstructed force appears clearly (Fig. 11).

6. Experimental validation

The method of reconstructing the force and the regularizing technique were experimentally validated. A cylinder of 1.75 m length, 0.4 m radius and 0.001 m thickness is posed vertically on the ground

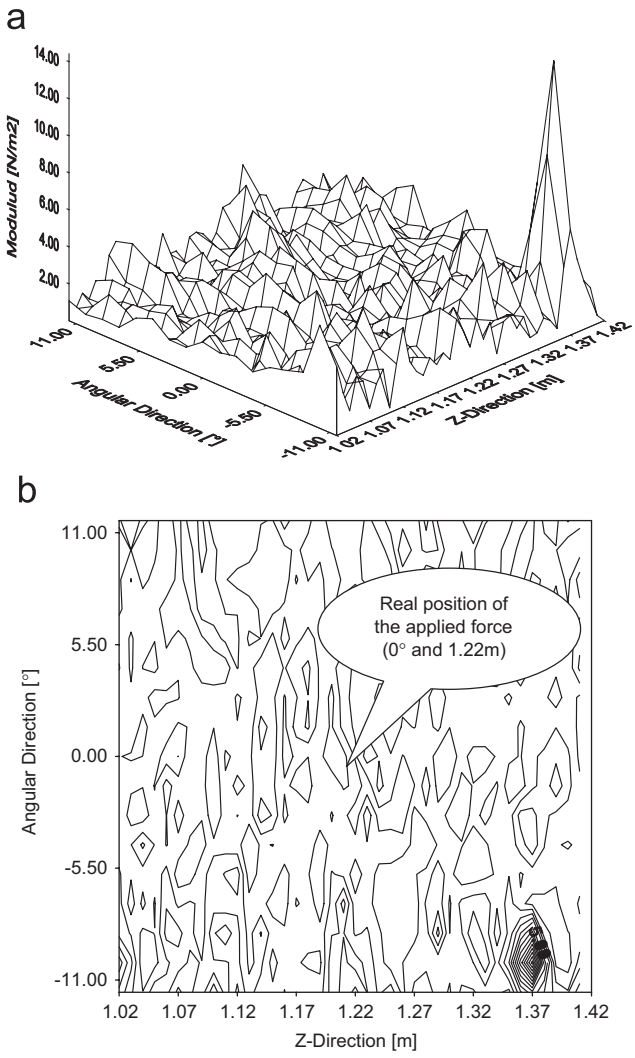

Fig. 13. Force distribution reconstructed from measurement data at 3200 Hz: (a) 3D presentation, (b) map contours.

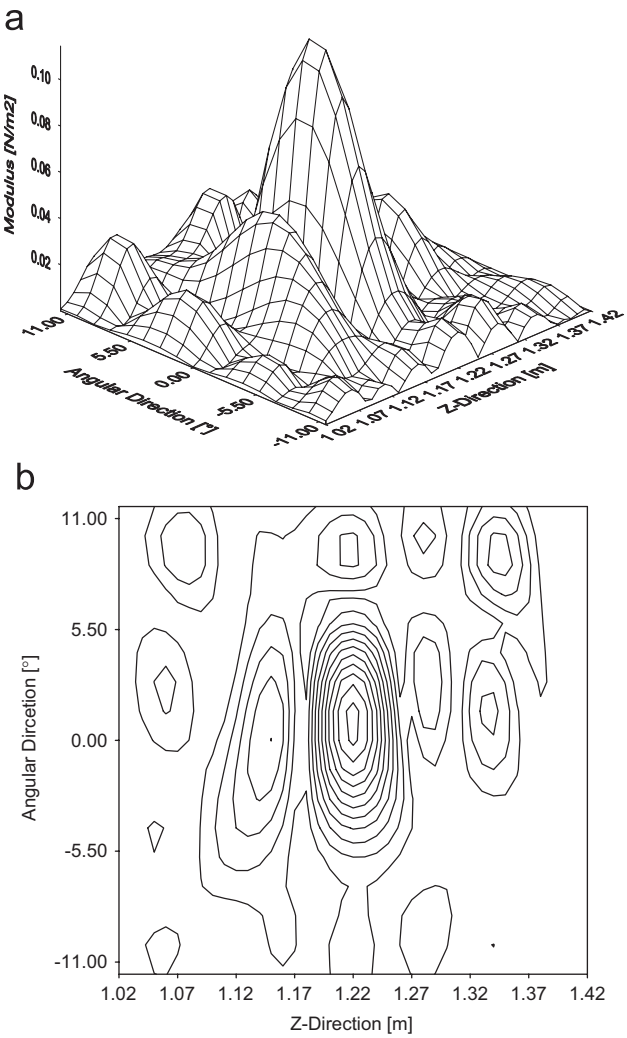

Fig. 14. Force distribution reconstructed after windowing and filtering at 3200 Hz with a cut-off wavenumber along both directions of 50 rad m^{-1}: (a) 3D presentation, (b) map contours.

(no displacement along the z-direction) and the second edge is free as shown in Fig. 12. The measurement system consists of a Polytec OFV056 optical scanning laser head and an OFV3001S Vibrometer controller connected to a PC. In order to excite the structure, a Shaker is placed inside the cylinder, roughly in the center of the scanning surface. The Laser head is placed at 1.8 m from the cylinder to measure the velocities on a selected surface of 0.20 m × 0.44 m. The scanning surface is divided into 945 points (21 points on the angular direction and 45 points along the axial direction).

Radial displacements introduced in Eq. (6) are calculated from the measured radial velocities. This is done without accounting for any deformations that may occur at the mesh points. As shown below, this assumption is true only above the ring frequency of the cylindrical shell ($\approx$2100 Hz). So a frequency of 3200 Hz is chosen for the validation of this experiment.

Fig. 13 represents the force distribution calculated from the measured data which show that the force position cannot be determined due to uncertainties resulting from the nonregular spacing between points on the measured surface. This ambiguity in determining the force is more pronounced for the curved surface where the spacing between data points along the edges of the scanned area is greater than the spacing between the data points near the center for the same scanning angle increment [17,18]. By applying the regularization method, the force appears clearly in the exact position as shown in Fig. 14.

7. Conclusion

The finite-difference method is used to identify the position of the force which excites a cylindrical shell from its internal side. At low frequencies, the knowledge of longitudinal and tangential deformations is necessary to achieve the reconstruction process of the input force. The measurement of these quantities by strain gauges is difficult but can be achieved when using a mesh with limited number of points. At frequencies that are equal or higher than the ring frequency, it is shown that it is possible to locate the force position from only the radial displacements. This is due to the vanishing of the coupling between radial and in-plane motion and hence making it easy to take measurements by a Scanning Laser Vibrometer for example. The proposed regularization technique gives positive results when using computer simulations as well as when performing experiments where measurements are taken with well-defined parameters. This confirms that the present method is convenient, effective and accurate.

References

[1] C.R. Fuller, Radiation of sound from an infinite cylindrical elastic shell excited by an internal monopole source, *Journal of Sound and Vibration* 109 (2) (1986).
[2] B. Laulagnet, J.L. Guyader, Sound radiated from finite cylindrical shells, partially covered with longitudinal strips of compliant layer, *Journal of Sound and Vibration* 186 (5) (1995) 723–742.
[3] N. Ouelâa, B. Laulagnet, J.L. Guyader, Etude vibro-acoustique d'une coque cylindrique finie remplie de fluide en mouvement uniforme, *Acta Acustica* 2 (1994) 275–289.
[4] J.R. Anthony, E.G. Williams, On the use of acoustical holography for the determination of intensity in structures, *Fourth International Congress on Intensity Techniques*, Senlis, France, 1993.
[5] Y. Zhang, J.A. Mann III, Measuring the structural intensity and force distribution in plates, *Journal of Acoustical Society of America* 99 (1996) 345–353.
[6] Y. Zhang, J.A. Mann III, Examples of using structural intensity and the force distribution to study vibrating plates, *Journal of Acoustical Society of America* 99 (1996) 353–361.
[7] A. Nedjade, R. Singh, Flexural intensity measurement on finite plates using modal spectrum ideal filtering, *Journal of Sound and Vibration* 256 (1) (2002) 33–63.
[8] M.D. Araújo, J. Antunes, P. Pitteau, Remote identification of impact forces on loosely supported tubes: part 1—basic theory and experiments, *Journal of Sound and Vibration* 215 (5) (1998) 1015–1041.
[9] S. Nakaggiri, K. Suzuki, Finite element analysis of external loads by displacement input with uncertainty, *Computer Methods in Applied Mechanics and Engineering* 168 (1999) 63–72.
[10] S.E.S. Karlsson, Identification of external structural loads from measured harmonic responses, *Journal of sound and vibration* 196 (1) (1996) 59–74.
[11] J.J. Liu, C.K. Ma, I.C. Kung, D.C. Lin, Input force identification of a cantilever plate by using a system identification technique, *Computer Methods in Applied Mechanics and Engineering* 190 (2000) 1309–1322.
[12] C. Pezerat, J.L. Guyader, Two inverse methods for localization of external sources exciting a beam, *Acta Acustica* 3 (1) (1995) 1–10.
[13] C. Pezerat, J.L. Guyader, Force analysis technique: reconstruction of force distribution on plates, *Acustica united with Acta Acustica* 86 (2000) 322–332.
[14] C. Pezerat, J.L. Guyader, Identification of vibration sources, *Applied Acoustics* 61 (2000) 309–324.
[15] M.C. Djamaa, N. Ouelaa, C. Pezerat, J.L. Guyader, Identification of external forces exciting finite thin cylindrical baffled shell, *International Conference on Noise and Vibration Engineering (ISMA2002)*, Leuven, Belgium, 2002.
[16] M.Y. Yang, G.H. Koopmann, An inverse method to compute equivalent forces on a structure based on sound power measurements, *Journal of Sound and Vibration* 252 (1) (2002) 65–82.
[17] W.X. Li, L.D. Mitchel, M.F. Lu, Using spatial DFT–IDFT techniques for mapping of non-square and unevenly spaced 2D velocity data acquired by scanning laser Doppler Vibrometer, *First International Conference on Vibration Measurements by Laser: Advances and Applications*, Ancona, Italy, 3–5 October 1994, Vol. 2358, SPIE, 1994, pp. 247–253.
[18] W. Bouber, D. Morton, C. Gedney, P. Abbot, Efficient system for wavenumber–frequency analysis of underwater structures, *Third International Conference on Vibration Measurements by Laser: Advances and Applications*, Ancona, Italy, 16–19 June 1998, Vol. 3411, SPIE, 1998, pp. 282–293.